optica

Is it possible to create a perfect fractional vortex beam?

GEORGIY TKACHENKO, MINGZHOU CHEN, KISHAN DHOLAKIA, AND MICHAEL MAZILU*

SUPA, School of Physics and Astronomy, University of St. Andrews, KY16 9SS, UK
**Corresponding author: michael.mazilu@st-andrews.ac.uk*

Received 26 October 2016; revised 6 February 2017; accepted 7 February 2017 (Doc. ID 279578); published 3 March 2017

Laguerre–Gaussian beams of integer azimuthal index satisfy the fundamental principle of quantization of orbital angular momentum. Here, we consider light-induced orbiting of a trapped microparticle as a probe of the local orbital angular momentum density in both integer- and fractional-index perfect vortex beams. Simulations suggest that the distribution and the corresponding light-induced motion of the particle may be uniform in beams with integer azimuthal index, but fundamentally this cannot be achieved in beams with fractional index. We experimentally verify these predictions by light-induced trapping and rotation of individual microparticles in fractional index beams where we distribute the phase dislocations around the annular profile.

OCIS codes: (050.4865) Optical vortices; (260.6042) Singular optics; (230.6120) Spatial light modulators; (350.4855) Optical tweezers or optical manipulation.

https://doi.org/10.1364/OPTICA.4.000330

The propagation of a monochromatic paraxial light field obeys the well-known paraxial wave equation. This equation has a direct correspondence to the Schrödinger equation for a free particle in 2D, with z replacing time, and the wavenumber, k, replacing mass divided by the reduced Planck's constant, $\hbar$. In cylindrical coordinates, the paraxial wave equation has a complete set of orthonormal solutions in the form of a Gaussian function multiplied by a Laguerre polynomial with a scale that varies with the transverse plane. The resultant Laguerre–Gaussian (LG) modes are characterized by two indices, ℓ (azimuthal) and p (radial). In effect, $2\pi\ell$ denotes the phase change experienced during a complete revolution of the azimuthal coordinate, θ, whereas $p+1$ defines the number of radial rings present in the intensity distribution. Here, we consider only single-ringed LG beams ($p = 0$). These solutions are eigenmodes of the orbital angular momentum (OAM) operator. Indeed, a key feature for the LG modes is that the OAM density is proportional to the local beam intensity. LG modes have gained increasing importance in the optical domain due to the fact that a beam with nonzero azimuthal index, ℓ, carries an on-axis singularity (or vortex) and an OAM equal to $\ell\hbar$ per photon [1].

Optical manipulation is a powerful route to probe LG beams [2]. The probing consists of observation of the light-induced orbiting of a microparticle that is trapped in the high intensity ring of an LG beam. The amount of OAM transferred to a microparticle is proportional to the ring size, the intensity, and the phase gradient (itself proportional to ℓ). However, using LG beams, it is not possible to maintain the same intensity profile while changing the azimuthal index. Recently, the concept of a "perfect optical vortex" was introduced, which allows one to construct an optical field with the OAM density being constant on a thin ring, with the radius of peak intensity independent of the ℓ number [3]. Such beams have been applied for trapping and propelling microparticles along the ring at a rate proportional to ℓ [4–6].

Further, one can superpose multiple LG modes of different azimuthal indices in order to generate a beam where the effective ℓ number is noninteger [7,8]. Such a fractional vortex beam has a helical phase of the form $\exp(i\ell\theta)$, with $\ell \in \mathbb{R}$. To ensure continuity of the optical fields, this beam must possess a phase dislocation, which inevitably leads to a distortion of the beam's intensity profile. It has been demonstrated that experimental imperfections of the intensity distribution in integer perfect vortex (PV) beams can be corrected in order to achieve constant azimuthal OAM density and, consequently, smooth optical manipulation [4,9]. In this Letter, we investigate whether a fractional PV beam can be made as smooth, in terms of the OAM density, as an integer one. To achieve this, we distribute the fractional phase discontinuity onto a number of smaller dislocations positioned periodically around the vortex. Ultimately, we aim at generalization of the "perfect optical vortex" concept to beams with fractional azimuthal indices. Our experimental approach relies on optomechanical probing of vortex fields by observing orbital motion of trapped mesoscale microparticles, which allows mapping of the local OAM density distributions [10–15]. In contrast to the common strategy of rotating "necklaces" of particles [4–6,16,17], which average over any intensity and phase irregularities of the field, here we probe integer and fractional vortices by means of *individual* microparticles.

Our experimental setup is sketched in Fig. 1. A phase-only liquid-crystal spatial light modulator (SLM; HSPDM512-1064, Boulder Nonlinear Systems, Inc.) is illuminated with a

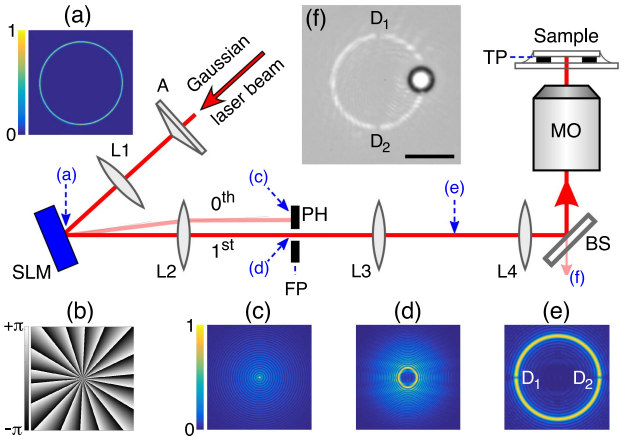

Fig. 1. Sketch of the experimental setup. (a) Measured intensity profile of the incident annular beam. (b) Phase mask on the SLM, corresponding to $\ell = 17.5$ with $N = 2$ distributed phase dislocations. (c)–(d) Simulated intensity profiles of the light sent to the zeroth and first diffraction orders. (e) Simulated intensity profile in the focal plane of lens L3, where the dark spots, D_1 and D_2, correspond to the above dislocations on the SLM. (f) Typical image of a bead and the PV ring. Scale bar is 10 μm.

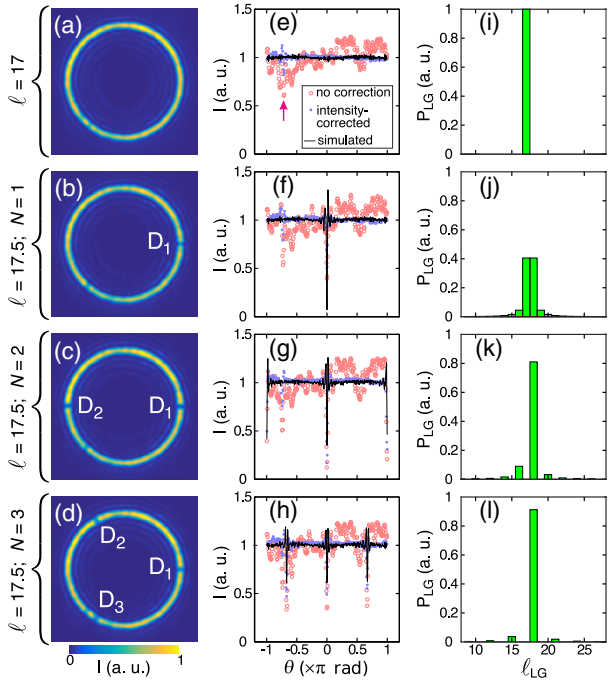

Fig. 2. (a)–(d) Experimental PV rings without intensity correction. (e)–(h) Intensity distribution along the azimuthal coordinate, θ: measured without correction (red markers); measured after intensity correction (blue markers); simulated (solid line). (i)–(l) Simulated decomposition of a fractional vortex beam into LG eigenmodes.

ring-shaped coherent light field [Fig. 1(a)] originating from a collimated laser beam (wavelength 1070 nm, waist 2.5 mm) after transmission through an axicon A (apex angle 178°) and lens L1 (focal length $f_1 = 0.2$ m). The SLM is used in the first diffraction order to encode the helical phase [Fig. 1(b)]. The light sent to the zeroth diffraction order [Fig. 1(c)] is blocked by the pinhole (PH) in the Fourier plane (FP) of lens L2 ($f_2 = 1$ m). The wavefront aberrations caused by the SLM are corrected in the FP [Fig. 1(d)] using the adaptive method described in [18]. The FP is relayed by lenses L3 and L4 ($f_{3,4} = 0.2$ m) to the back focal plane of the microscope objective (MO; 40 ×, NA = 1.3, oil immersion). The PV beam is created in the trapping plane (TP) inside a sealed glass cell containing spherical polystyrene beads (Polyscience, Inc.) immersed in heavy water. The TP is imaged via the MO using a dichroic beam splitter (BS), a lens, and a CMOS camera. Typical image of the PV beam and a trapped bead is shown in Fig. 1(f).

The bead is trapped on the PV ring by gradient optical forces and pressed to the top glass slide by scattering ones. The bead is set into rotation along the PV ring circumference under the action of azimuthal optical forces, which originate from scattering and are proportional to the local density of the OAM of the light. The angular speed is proportional to the optical power P and the local phase gradient, which (for a smooth helical phase profile) scales with the azimuthal index, ℓ. In practice, individual beads start orbiting when the absolute value of ℓ is large enough to overcome friction and Brownian motion. Moreover, we have observed degradation of experimental samples, meaning that the angular motion of beads gradually slows down and ceases within a few hours. Therefore, in the present study, we used $|\ell| > 15$ in order to accelerate the measurements. The azimuthal index is limited only by the resolution of the SLM and nowadays can easily exceed 100, but the increase of $|\ell|$ results in broadening of the higher-order Bessel beam in the FP, so the field of larger $|\ell|$ is more strongly clipped by apertures in the optical system. In this study, we use $|\ell| < 20$.

Theoretically, integer ℓ values correspond to beams with intensity profiles independent of the azimuth, θ. The solid line in Fig. 2(e) is the azimuthal dependence of a PV intensity obtained by a paraxial simulation of the field with $\ell = 17$ propagated through the system (the PH aperture radius was taken as 15% of the radius of the annular illumination impinging on the SLM).

In practice, however, the observed intensity versus θ is far from uniform, as one can see in Fig. 2(a), which presents a PV beam of $\ell = 17$ captured in the focal plane of L3. These azimuthal variations are primarily caused by the unavoidable asymmetry of the laser beam illuminating the axicon and by imperfections of the axicon itself. In order to smooth out the intensity and thus move toward more uniform rotation of beads in the experiment, we apply a correction algorithm based on adjusting the local diffraction efficiency of the blazed grating on the SLM [4]. The intensity distributions before (red markers) and after (blue markers) the intensity correction are presented in Fig. 2(e). It is noteworthy that one narrow region (indicated by the arrow) still shows a marked disturbance. This is a result of the destructive interference between the PV ring and the light sent by the SLM to the zeroth diffraction order.

The local intensity minimum produced by the phase dislocation in the case $\ell = 17.5$ is denoted by D_1 in Fig. 2(b). Even after the correction, the intensity profile still shows significant nonuniformity around the phase dislocation, as seen in Fig. 2(f). In fact, the correction algorithm cannot increase the intensity at D_1, since the dark spot appears due to a phase singularity.

As mentioned above, a paraxial PV beam can be conveniently represented as a series of $LG_{\ell p}$ eigenmodes [8]. Since perfect vortices are restricted to a single light ring, one can drop the radial

index: $p = 0$. Within this decomposition, the amplitude of the OAM eigenstates corresponds to the amount this integer valued OAM mode contributes to the fractional PV beam.. These OAM states form a complete orthonormal basis, hence the net probability, $\sum P_{LG} = \sum |p_{LG}|^2$, of the beam to carry the average OAM of $\ell\hbar$ per photon is unity.

Let us denote the closest integer number to ℓ as ℓ_{int}. For an integer vortex beam, we have $\ell = \ell_{int}$, and the OAM distribution is confined to the single mode with $\ell_{LG} = \ell_{int}$, as shown in Fig. 2(i), where the calculated probability, P_{LG}, is plotted against the OAM eigenstates. When $\mu = |\ell - \ell_{int}|$ increases, the probability for the neighboring LG mode with index $(\ell_{int} \pm 1)$ increases at the expense of the probability for the mode with index ℓ_{int}, and the two probabilities are equalized when $\mu = 0.5$; see Fig. 2(j). Therefore, a PV beam with a half-integer ℓ number must give the largest disturbance of the angular speed of a particle trapped and rotating along the ring. In practice, we usually found a probe bead to stop at D_1 in this case.

In order to reduce the intensity and phase disturbances of a fractional vortex beam without altering the net OAM, we distribute the phase dislocation along the SLM, producing N smaller dislocations, D_1, D_2, ...D_N. The phase mask for the SLM is defined as

$$\phi(\ell, \theta) = \ell_{int}\theta + (\ell - \ell_{int})[\theta \bmod (2\pi/N)], \quad (1)$$

where mod is the remainder of division. When the phase profile has N dislocations, as shown in Figs. 2(j)–2(l), the probability, P_{LG}, peaks at ℓ_{int}, and the OAM distribution consists only of the modes with indices $(\ell_{int} + NK)$, where $K \in \mathbb{Z}$. In terms of the intensity profiles, both experimental [see Figs. 2(b)–2(d) and markers in Figs. 2(f)–2(h)] and theoretical [solid lines in Figs. 2(f)–2(h)] data confirm that the fractional PV ring becomes smoother as the number of dislocations, N, is increased.

Based on the above result, one might wish to further increase N in order to produce a fractional vortex ring of almost homogeneous intensity. However, the resolution of adjacent dislocations is practically limited by the pixel size of the SLM and fundamentally limited by the wavelength of light (dislocations closer than the wavelength decay evanescently and do not propagate). Therefore, it is not possible to create arbitrary smooth fractional PV beams. In our experiments, the PV ring radius, R_{PV}, is about 10 μm (it can be a few times larger at the expense of intensity, which is crucial for the optomechanical study); hence, with the given laser wavelength, we use $N \leq 10$.

Prior to the experimental optomechanical probing, we simulate the expected OAM transfer to a dielectric particle placed in a fractional vortex beam. The particle's orbital angular momentum, L, at each azimuthal position, θ, is considered proportional to the local phase gradient and intensity level. Figure 3(a) shows how the normalized standard deviation of the local OAM, ΔL, varies with the azimuthal index, ℓ. As expected, ΔL demonstrates a periodical behavior with maxima located at half-integer ℓ values. As presented in Fig. 3(b), distribution of the phase disturbance by multiple $(N > 1)$ dislocations does decrease the variation of local OAM in a fractional vortex beam. The dependence $\Delta L(N)$ peaks at $N = 2$ (although one could expect the maximum disturbance of the vortex field to occur for $N = 1$) and then decreases exponentially. The simulation results are summarized in Fig. 3(c); see Fig. S1 for higher ℓ values.

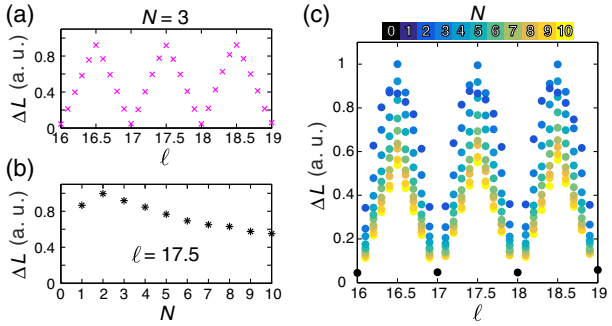

Fig. 3. Numerically simulated nonuniformity of the local OAM, L, in a PV beam. ΔL is the normalized standard deviation of L as a function of (a) the azimuthal index, ℓ, in the case of three distributed phase dislocations, $N = 3$, (b) the number of phase dislocations, N, for a fixed azimuthal index $\ell = 17.5$, and (c) ℓ for a different number of phase dislocations, N.

When proceeding to the optomechanical experiment, we are facing the following geometrical trade-off. The trapped particle must have a measurable light-induced angular speed, which, in a viscous environment, scales as the particle's radius, R. At the same time, we need to minimize the particle's chaotic Brownian motion, which causes random displacements proportional to $1/R$. Consequently, the particle shall be as large as possible, given it still can resolve the local phase disturbances of the PV ring. Further, we remark that the finite particle size plays a role in the observed dynamics, as it averages over the local OAM variations present in the beam. As such, larger particles are less sensitive to distributed phase dislocations. Based on these considerations and the experimental evidence, we have come to the following set of parameters for the study: the PV ring has radius $R_{PV} \approx 18$ μm in the trapping plane; ℓ ranges from 17 to 18 with an increment of 0.1; the phase disturbance in a fractional PV is distributed by $N \leq 8$ dislocations; the PH opening diameter is around 2 mm; and, the particle's diameter is 5 μm ± 0.3 μm.

We measured the angular speed, $\Omega(\theta)$, of a polystyrene bead trapped and driven by the PV beam with optical power $P \approx 0.22$ W (at the back aperture of the MO). Typical mean angular speed $\bar{\Omega}$ measured about 0.6 rads^{-1} and 0.9 rads^{-1} before and after the amplitude correction, respectively. Since in this study we focus on the OAM in vortex beams, the bead's angular speed is expressed in the units of OAM following $L(\theta) = mR_{PV}\Omega(\theta)$, where m is the bead's mass. Two representative sets of data are presented in Fig. 4, where the standard deviation ranges of $L(\theta)$ are shown as gray areas. As expected, the integer vortex beam [Fig. 4(a)] provides smoother light-induced orbiting than the fractional vortex beam [Fig. 4(b)].

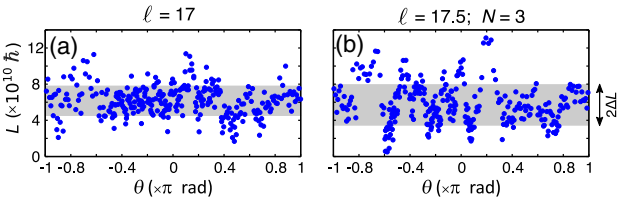

Fig. 4. Measured local OAM, $L(\theta)$, of a trapped microparticle driven by an intensity-corrected PV beam (a) with $\ell = 17$ and (b) with $\ell = 17.5$ and $N = 3$ phase dislocations. Markers, experimental data; gray areas, standard deviation ranges $(2\Delta L)$.

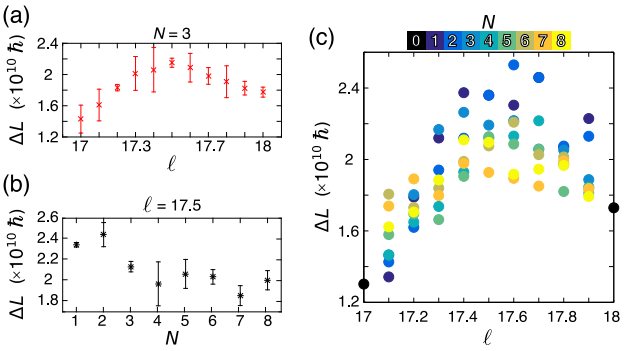

Fig. 5. Experimental probing of the local OAM density in integer and fractional PV beams. Standard deviation of the OAM of an optically rotated particle is plotted as a function of (a) the azimuthal index, ℓ, (b) the number of phase dislocations, N. (c) Full data set for one particle.

The measured dependences of ΔL on ℓ and N approximately follow the theoretical trends shown in Figs. 3(a) and 3(b). Namely, the local OAM becomes less regular around the half-integer ℓ value, as opposed to the integer values [Fig. 5(a)]; for a given fractional ℓ, the OAM variation takes the maximum value at $N = 2$ and gradually decreases for higher numbers of phase dislocations [Fig. 5(b)]. The error bars are obtained from three independent sets of data points. One data set is presented in full in Fig. 5(c), where each point corresponds to a 10 s long video. Acquisition of the data set took about 1 h. As such, experimental results were affected by the sample deterioration mentioned previously. In our measurements, ℓ was increased with time, which explains a higher ΔL value at $\ell = 18$, when compared to that at $\ell = 17$.

In conclusion, we have reported on the generation and optomechanical probing of vortex beams with helical phase profiles characterized by fractional azimuthal indices. The optical fields were created in the form of PV beams using a phase-only SLM. Paraxial simulations predict that a fractional-indexed vortex beam must possess a phase and intensity disturbance, which does not allow the achievement of an azimuthal distribution of OAM density that is as smooth as in an integer-indexed beam. In fact, a fractional vortex cannot be completely smoothed out by distributing the phase dislocation over the beam profile without changing the net OAM of light. Answering the question posed in the title of this letter, this means that one cannot create perfect fractional vortex beams. This statement is confirmed experimentally by probing of the local OAM density using individual dielectric microparticles that are optically trapped and propelled around a PV beam circumference. Although our experimental approach considers a macroscopic system, the observed effect is a manifestation of the quantization of the OAM of light. We believe that our results deliver an important message for the major areas where OAM of light is applied, namely optical manipulation [2], quantum information [19], and optical communication [20].

Datasets and scripts can be accessed at Ref. [21].

Funding. Engineering and Physical Sciences Research Council (EPSRC) (EP/J01771X/1, EP/M000869/1).

See Supplement 1 for supporting content.

REFERENCES

1. L. Allen, M. W. Beijersbergen, R. J. C. Spreeuw, and J. P. Woerdman, Phys. Rev. A **45**, 8185 (1992).
2. M. Padgett and R. Bowman, Nat. Photonics **5**, 343 (2011).
3. A. S. Ostrovsky, C. Rickenstorff-Parrao, and V. Arrizón, Opt. Lett. **38**, 534 (2013).
4. M. Chen, M. Mazilu, Y. Arita, E. M. Wright, and K. Dholakia, Opt. Lett. **38**, 4919 (2013).
5. J. García-García, C. Rickenstorff-Parrao, R. Ramos-García, V. Arrizón, and A. S. Ostrovsky, Opt. Lett. **39**, 5305 (2014).
6. R. Paez-Lopez, U. Ruiz, V. Arrizón, and R. Ramos-García, Opt. Lett. **41**, 4138 (2016).
7. W. M. Lee, X.-C. Yuan, and K. Dholakia, Opt. Commun. **239**, 129 (2004).
8. J. B. Götte, S. Franke-Arnold, R. Zambrini, and S. M. Barnett, J. Mod. Opt. **54**, 1723 (2007).
9. M. Chen, M. Mazilu, Y. Arita, E. M. Wright, and K. Dholakia, Opt. Rev. **22**, 162 (2015).
10. N. B. Simpson, K. Dholakia, L. Allen, and M. J. Padgett, Opt. Lett. **22**, 52 (1997).
11. M. E. J. Friese, T. A. Nieminen, N. R. Heckenberg, and H. Rubinsztein-Dunlop, Nature **394**, 348 (1998).
12. A. T. O'Neil, I. MacVicar, L. Allen, and M. J. Padgett, Phys. Rev. Lett. **88**, 053601 (2002).
13. V. Garcés-Chávez, K. Volke-Sepulveda, S. Chávez-Cerda, W. Sibbett, and K. Dholakia, Phys. Rev. A **66**, 063402 (2002).
14. V. Garcés-Chávez, D. McGloin, M. J. Padgett, W. Dultz, H. Schmitzer, and K. Dholakia, Phys. Rev. Lett. **91**, 093602 (2003).
15. V. Garcés-Chávez, D. McGloin, M. D. Summers, A. Fernandez-Nieves, G. C. Spalding, G. Cristobal, and K. Dholakia, J. Opt. A **6**, S235 (2004).
16. K. T. Gahagan and G. A. Swartzlander, Opt. Lett. **21**, 827 (1996).
17. J. E. Curtis and D. G. Grier, Phys. Rev. Lett. **90**, 133901 (2003).
18. T. Čižmár, M. Mazilu, and K. Dholakia, Nat. Photonics **4**, 338 (2010).
19. G. Molina-Terriza, J. P. Torres, and L. Torner, Nat. Phys. **3**, 305 (2007).
20. A. E. Willner, H. Huang, Y. Yan, Y. Ren, N. Ahmed, G. Xie, C. Bao, L. Li, Y. Cao, Z. Zhao, J. Wang, M. P. J. Lavery, M. Tur, S. Ramachandran, A. F. Molisch, N. Ashrafi, and S. Ashrafi, Adv. Opt. Photon. **7**, 66 (2015).
21. G. Tkachenko, M. Chen, K. Dholakia, and M. Mazilu, University of St. Andrews (2017), http://dx.doi.org/10.17630/49bd9620-2d38-4a50-a950-591b5a3fb578.